

Geophysical Research Letters



RESEARCH LETTER

10.1029/2019GL084566

Key Points:

- The 2018 active tropical cyclone season in the North Pacific was successfully predicted 5 months in advance
- The subtropical Pacific warming in 2018 mainly caused the active storm season in the North Pacific
- The potential effect of anthropogenic forcing on the 2018 active storm season is uncertain

Supporting Information:

- Supporting Information S1

Correspondence to:

H. Murakami and P.-C. Hsu,
 hir.murakami@gmail.com;
 pangchi@nuist.edu.cn;
 pangchi.hsu@gmail.com

Citation:

Qian, Y., Murakami, H., Nakano, M., Hsu, P.-C., Delworth, T. L., Kapnick, S. B., et al. (2019). On the mechanisms of the active 2018 tropical cyclone season in the North Pacific. *Geophysical Research Letters*, 46, 12,293–12,302. <https://doi.org/10.1029/2019GL084566>

Received 15 JUL 2019

Accepted 15 SEP 2019

Accepted article online 9 OCT 2019

Published online 3 NOV 2019

On the Mechanisms of the Active 2018 Tropical Cyclone Season in the North Pacific

Y. Qian^{1,2,3} , H. Murakami^{2,4,5} , M. Nakano⁶ , P.-C. Hsu¹ , T. L. Delworth^{2,3} , S. B. Kapnick² , V. Ramaswamy^{2,3} , T. Mochizuki^{6,7} , Y. Morioka⁶ , T. Doi⁶ , T. Kataoka⁶ , T. Nasuno⁶ , and K. Yoshida⁵

¹Key Laboratory of Meteorological Disaster of Ministry of Education, Nanjing University of Information Science and Technology, Nanjing, China, ²National Oceanic and Atmospheric Administration/Geophysical Fluid Dynamics Laboratory, Princeton, NJ, USA, ³Atmospheric and Oceanic Sciences Program, Princeton University, Princeton, NJ, USA, ⁴University Corporation for Atmospheric Research, Boulder, CO, USA, ⁵Meteorological Research Institute, Tsukuba, Japan, ⁶Japan Agency for Marine-Earth Science and Technology, Yokohama, Japan, ⁷Department of Earth and Planetary Sciences, Faculty of Science, Kyushu University, Fukuoka, Japan

Abstract The 2018 tropical cyclone (TC) season in the North Pacific was very active, with 39 tropical storms including eight typhoons/hurricanes. This activity was successfully predicted up to 5 months in advance by the Geophysical Fluid Dynamics Laboratory Forecast-Oriented Low Ocean Resolution (FLOR) global coupled model. In this work, a suite of idealized experiments with three dynamical global models (FLOR, Nonhydrostatic Icosahedral Atmospheric Model, and Meteorological Research Institute Atmospheric General Circulation Model) was used to show that the active 2018 TC season was primarily caused by warming in the subtropical Pacific and secondarily by warming in the tropical Pacific. Furthermore, the potential effect of anthropogenic forcing on the active 2018 TC season was investigated using two of the global models (FLOR and Meteorological Research Institute Atmospheric General Circulation Model). The models projected opposite signs for the changes in TC frequency in the North Pacific by an increase in anthropogenic forcing, thereby highlighting the substantial uncertainty and model dependence in the possible impact of anthropogenic forcing on Pacific TC activity.

Plain Language Summary The potential causes of the active 2018 tropical cyclone season in the North Pacific were explored with a series of high-resolution climate model experiments, revealing that this active cyclone season was mainly induced by subtropical Pacific warming and secondarily by tropical Pacific warming. The possible effect of anthropogenic forcing on the active cyclone season was also investigated. However, diverse results were obtained regarding projected changes in storm frequency in the case of an increase in anthropogenic forcing, thereby highlighting the substantial uncertainty in the possible impact of anthropogenic forcing on the 2018 active cyclone season.

1. Introduction

The 2018 tropical cyclone (TC) season (July–November) in the North Pacific was highly active. Among the 39 tropical storms (maximum surface wind speed ≥ 17.5 m/s) observed over the North Pacific in the 2018 TC season, eight storms became Category 5 super storms (maximum surface wind speed ≥ 70.6 m/s) and 21 out of 39 TCs made landfall (Figure 1a), causing substantial widespread damage to the coastal regions of East Asia, the Hawaiian Islands, the southwestern United States, and Mexico. The observed storm days (SDAYs; the total number of TC days throughout the lifetimes of TCs; Wang et al., 2010), an index used to measure the basin-wide TC activity, was 228.3 days for the 2018 TC season, exceeding 1.1 standard deviations above the climatological mean during 1980–2017 (Figure 1b).

El Niño–Southern Oscillation is thought to be one of the most important factors modulating the interannual variability of TC activity in the North Pacific. During El Niño developing years, TCs generate more frequently than during neutral and La Niña years over the southeastern quadrant of the western North Pacific (WNP) and tropical Central Pacific (CP). TCs tend to propagate northwestward with longer duration and a stronger intensity, causing a larger SDAY value than during neutral and La Niña years (Camargo & Sobel, 2005; Chan, 2007; Clark & Chu, 2002; Wang et al., 2010; Wang & Chan, 2002). The 2018 TC season was characterized by moderate El Niño conditions with a +0.49 standard deviation for the Niño 3.4 index

©2019. The Authors.

This is an open access article under the terms of the Creative Commons Attribution License, which permits use, distribution and reproduction in any medium, provided the original work is properly cited.

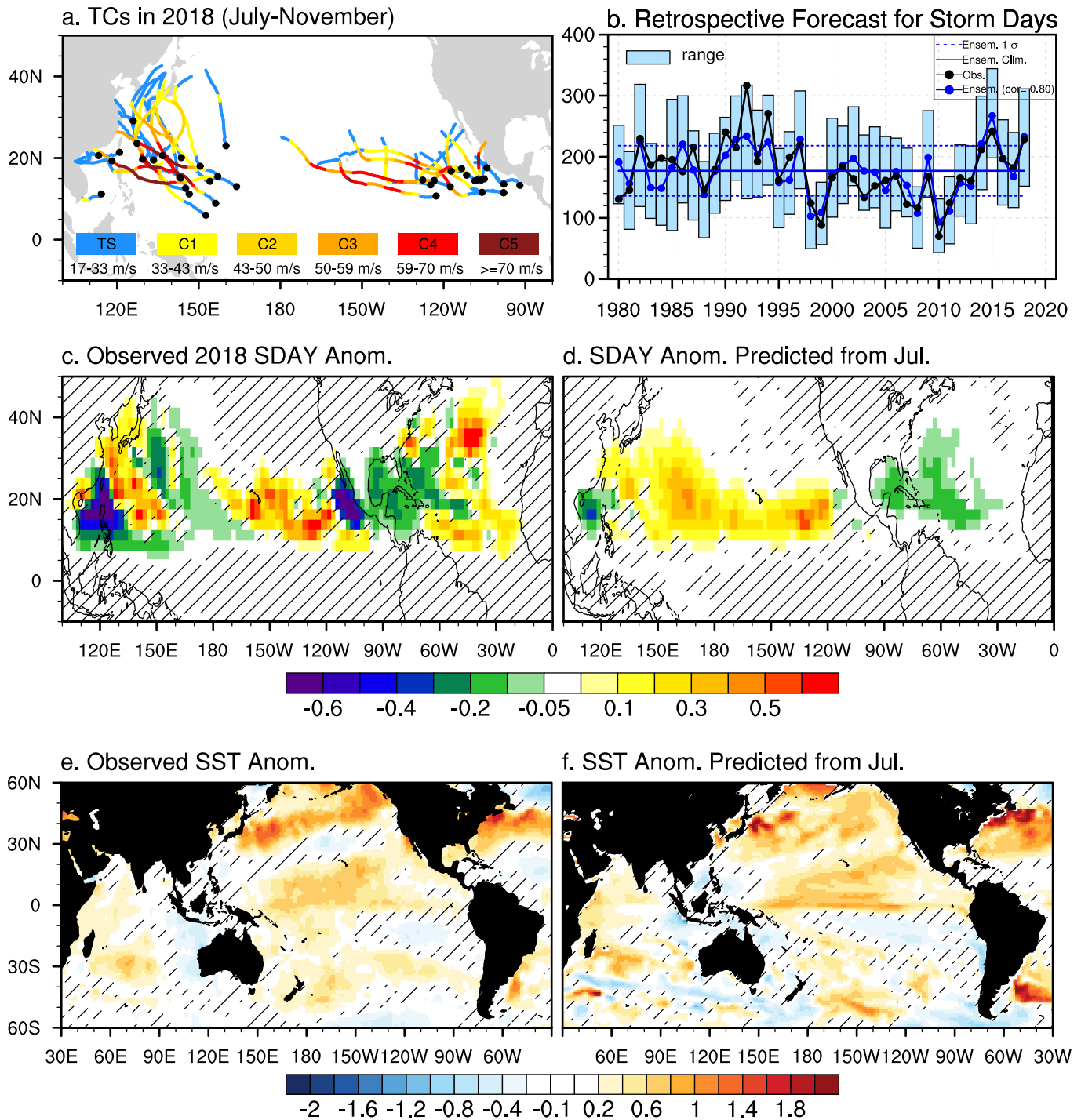


Figure 1. Observed and predicted TCs, SDAYs, and SSTs in 2018. (a) Observed TCs during the 2018 TC season (July–November). TC tracks are colored according to the intensities of the TCs, as categorized by the Saffir–Simpson hurricane wind scale (tropical storm; C1–C5, Category 1 to 5 hurricane intensity). (b) Observed (black) and predicted ensemble mean (blue thick line) of SDAY (days) during the TC seasons of 1980–2018 along with the maximum and minimum ranges among the ensemble members (light blue bars). Predictions were initialized on 1 July for each year. Dashed and solid blue lines represent the ensemble mean climatology and one standardized deviation from the climatology, respectively. (c, d) Observed and predicted SDAY anomalies (days) counted for each 2.5×2.5 grid cell during the 2018 TC season. (e, f) As in (c, d) but for SST anomalies (K). Hashed areas in the panels indicate that the anomalies relative to the climatological mean on grid cells are not statistically significant at the 95% confidence level (bootstrap method proposed by Murakami et al., 2013). TC = tropical cyclone; SDAY = storm day; SST = sea surface temperature.

(the area-averaged sea surface temperature anomaly [SSTA] in 5°S to 5°N, 170–120°W). Importantly, the peak of the SSTA observed during the 2018 TC season was located in the tropical CP rather than in the eastern tropical Pacific (Figure 1e), a characteristic of the so-called CP El Niño or El Niño Modoki (Ashok & Yamagata, 2009). Indeed, the observed El Niño Modoki index (Ashok & Yamagata, 2009) had a standard deviation of nearly +1.0 during the 2018 TC season (data not shown). Previous studies reported that CP El Niño can induce substantial increases in TC duration and intensity in the WNP (Hong et al., 2011; Patricola et al., 2018), implying that the 2018 CP El Niño could have been a key factor for the active 2018 TC season in the North Pacific as well as the WNP.

In addition to the CP El Niño, marked warming in the subtropical Pacific (7.5–27°N, 150°E to 120°W) was also observed during the 2018 TC season, partially associated with a positive phase of the Pacific Meridional Mode (PMM; Chiang & Vimont, 2004; Figure 1e) and may have been another potential factor for the active 2018 TC season in the North Pacific. The close relationship between TCs and the PMM has been identified in previous studies (Gao, et al., 2018; Murakami et al., 2017; Zhang et al., 2016); more TCs in the WNP and CP occur during the positive PMM phase. Although the PMM and CP El Niño cannot be considered as independent dynamical phenomena owing to their close linkage (Chang et al., 2007; Lorenzo et al., 2015; Stuecker, 2018), it is unclear which of the warm conditions—in the tropical or subtropical Pacific—caused the active 2018 TC season.

In this work, the physical mechanisms behind the active 2018 TC season in the North Pacific were explored. First, a suite of model simulations was analyzed to understand the effect of regional SSTAs on the 2018 TC activity in the North Pacific. Then, the possible impact of anthropogenic forcing on TC activity in the North Pacific was investigated using two dynamical models. Following this introduction, section 2 describes the observed data and models used in this study, section 3 reports the results, and section 4 provides a summary and discussion of the results.

2. Data

2.1. Observed Data

The TC data were obtained from the U.S. Department of Defense Joint Typhoon Warning Center Best Track Database, as archived in the International Best Track Archive for Climate Stewardship (Knapp et al., 2010), for the period 1980–2017. The 2018 data were complemented in this study by the operational best track data openly available in the global repository compiled through the Tropical Cyclone Guidance Project (2019). The sea surface temperature (SST) of the UK Met Office Hadley Centre SST product (Rayner et al., 2003) was used as the observed SST for the period 1980–2018. Monthly data of relative vorticity at 850 hPa from the Japanese 55-year Reanalysis (Kobayashi et al., 2015) were also employed.

2.2. Models

Three models were used in this work to avoid a dependency of the model results on the model choice. The first was the Geophysical Fluid Dynamics Laboratory Forecast-Oriented Low Ocean Resolution (FLOR) version of the Geophysical Fluid Dynamics Laboratory Coupled Model, version 2.5 (CM2.5; Delworth et al., 2012; Vecchi et al., 2014). FLOR's atmosphere and land components (50 × 50 km) are obtained from CM2.5, while its ocean component (1° × 1°) is taken from CM2.1 (Delworth et al., 2006). The second model was the 60-km-mesh Meteorological Research Institute (MRI) Atmospheric General Circulation Model (MRI-AGCM), version 3.2 (Mizuta et al., 2012; Murakami, Mizuta, et al., 2012; Murakami, Wang, et al., 2012; Yoshida et al., 2017), which was developed by the Japan Meteorological Agency and MRI. The third model was the 14-km-mesh Nonhydrostatic Icosahedral Atmospheric Model (NICAM) developed at the Japan Agency for Marine-Earth Science and Technology, University of Tokyo, and Riken (Miura et al., 2007; Nakano et al., 2015; Satoh et al., 2008; Satoh et al., 2014; Yamada et al., 2017; Yamada et al., 2019), which configures a global cloud-resolving model and adopts nonhydrostatic governing equations and icosahedral grids. Some of the experiments were not conducted with NICAM (supporting information Table S1) owing to limited computational resources.

3. Results

3.1. Successful Predictions for the Active 2018 TC Season

The FLOR seasonal forecast system (see details in Text S1) demonstrated skill in predicting the active 2018 North Pacific TC season initialized on 1 July 2018 (Figures 1b and 1d). The predicted seasonal (July–November) SDAY value from the 2018 July initial forecasts was 232.8 days (+1.4 standard deviations), which was close to the corresponding observed value (228.3 days, Figure 1b). The observed SDAY values in other years were also predicted well in the retrospective seasonal forecasts initialized from 1 July for each year during 1980–2018 (Figure 1b). The temporal correlation coefficient between the predicted and observed SDAYS was 0.80 for the period 1980–2018 (Figure 1b), exceeding the 99% significance level with a *t* test. The SDAY anomalies counted in each $2.5^\circ \times 2.5^\circ$ grid cell predicted by FLOR initiated from the 1 July 2018 initial forecasts (Figure 1d) were compared with observed values (Figure 1c). The observed 2018 SDAY spatial anomaly patterns were generally well predicted by the real-time predictions with FLOR. The observed positive anomaly in the WNP and CP and negative anomaly in the South China Sea and Gulf of Mexico were well predicted by FLOR. However, there were some discrepancies between the predictions and observations insofar as the observed negative anomalies southeast of Japan were missing in the predictions. An accurate prediction of SSTAs is necessary (but not sufficient) for an accurate prediction of TC activity. The predicted SSTAs for the 2018 TC season by FLOR (Figure 1f) showed similar spatial patterns to observations (Figure 1e). The marked positive SSTAs were found in both the subtropical Pacific and tropical CP in the predictions, although there were some differences in the magnitude and peak location of the SSTAs. Unlike the typical limitations in skill of seasonal predictions made before April initial forecasts (Duan & Wei, 2013; Murakami et al., 2018), the active TC season and SSTAs in 2018 were successfully predicted by FLOR at three to five lead months (predictions initialized on 1 April, 1 March, and 1 February; Figure S1). The positive SSTAs in the WNP near Japan, the subtropical Pacific, and the tropical CP were also well predicted, even by the three to five lead-month forecasts.

3.2. Assessing the Physical Mechanisms Behind the Active 2018 TC Season

To clarify the relative importance of the different regional SSTAs for the active 2018 TC season in the North Pacific, a series of idealized seasonal-prediction experiments were conducted with 12 ensemble members using each of the three independent dynamical models. Following Murakami et al. (2018), the SSTs in the idealized predictions were restored to the SSTs that were derived from the original real-time seasonal predictions initialized on 1 July 2018 by FLOR with some modifications. A series of different prescribed idealized SST experiments were conducted to investigate the impact of regional SSTAs on SDAY anomalies in the North Pacific. We also evaluated the accumulated cyclone energy (Bell et al., 2000), and the conclusions were qualitatively consistent with those based on SDAY (Figure S2), although models underestimated accumulated cyclone energy owing to their low resolution to simulate intense storms. Details of the prescribed idealized regional SST experiments are provided in Text S2 and summarized in Table S1. The left-hand column in Figure 2 shows the six different prescribed SSTA patterns. The resultant multimodel ensemble means of SDAY anomalies predicted by the dynamical models are shown in the right-hand column in Figure 2, and those by individual models are shown in Figure S3. As a reference experiment, referred to as CLIM, the SSTs were restored to the predicted climatological mean SSTs computed from the real-time predictions by FLOR over the period 1982–2012 to represent the present-day mean state. In the second experiment, the SSTs, in which the 2018 SSTAs predicted by the FLOR real-time prediction (i.e., Figure 1f) were superimposed on the CLIM SSTs, were restored. This experiment was named CLIM+ (Figure 2a). Note that the predicted SSTAs were used rather than the observed SSTAs as the lower boundary conditions for the idealized experiments, because the observed SSTAs for the 2018 summer season were unavailable when the study commenced. We confirmed that the consistent results were obtained even using the observed SSTAs (Text S2). The CLIM+ experiments showed active TCs over almost the entire North Pacific Ocean, except in the South China Sea and eastern North Pacific (right-hand panel of Figure 2a). The simulated SDAY values accumulated over the entire North Pacific by CLIM+ were much higher than those by CLIM (Figure 3), all exceeding the 95% significance level, and were similar to the values produced by the real-time predictions of FLOR. The similarity in the higher SDAY values over the tropical CP between the real-time predictions (Figure 1d) and CLIM+ experiments (Figure 2a) highlights the low dependency of the results on

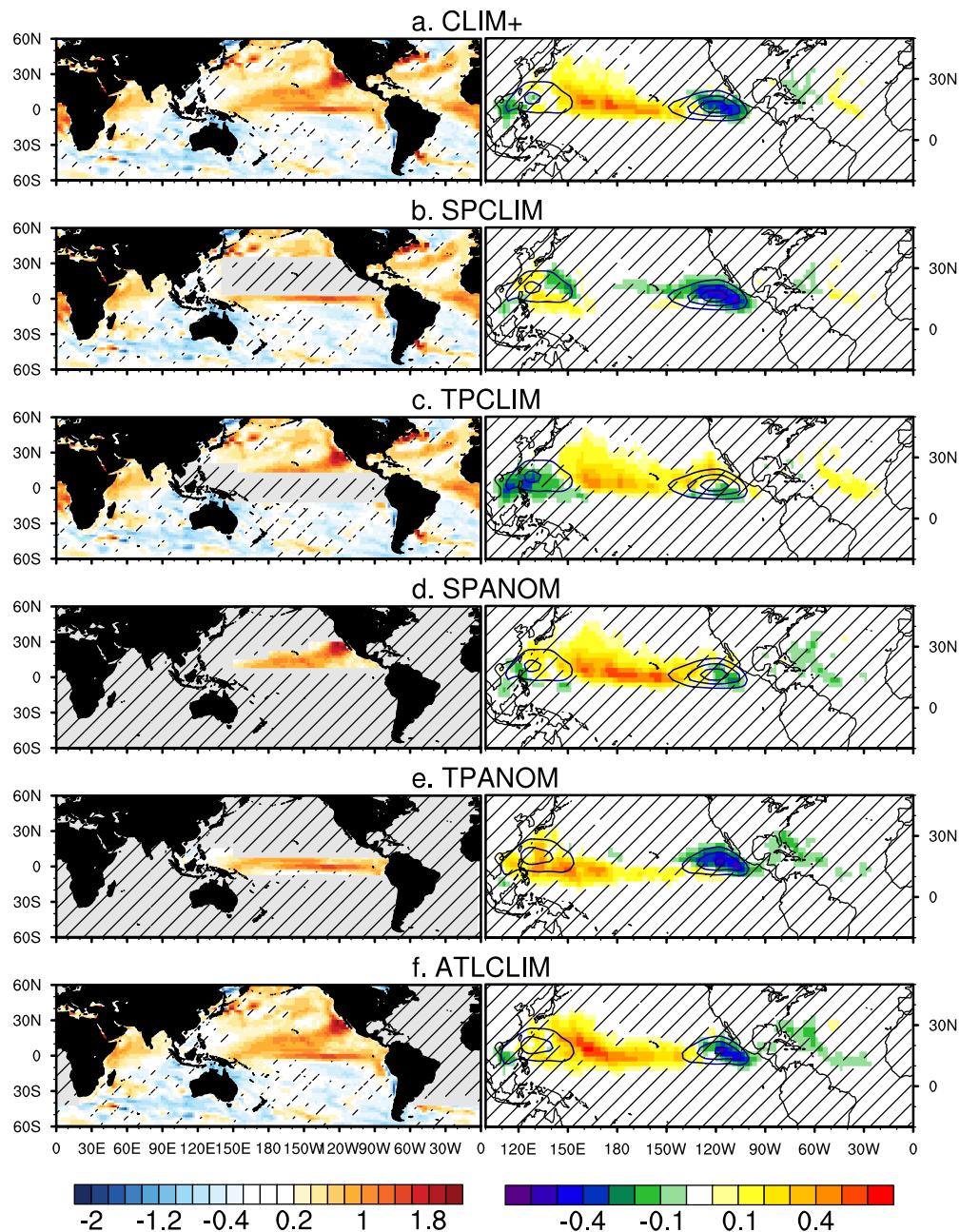


Figure 2. Prescribed idealized sea surface temperature (SST) anomaly (SSTA) and predicted storm day anomaly during the tropical cyclone season. Idealized seasonal forecasts conducted by prescribing the idealized SSTs in which SSTAs (shading; left-hand panels; units: kelvins) are superimposed on the climatological mean SST (CLIM). The resultant predicted multimodel ensemble mean of SDAY anomalies relative to the CLIM experiment are shown by the shading, and the CLIM experiment is shown by the contours in the right-hand panels (units: days per season; contour interval = 0.4 days per season from 0). The prescribed SSTAs are (a) all 2018 anomalies (CLIM+); (b) as in CLIM+ except the SSTAs in the subtropical Pacific are replaced with CLIM (SPCLIM); (c) as in CLIM+ except the SSTAs in the tropical Pacific are replaced with CLIM (TPCLIM); (d) only the SSTAs in the subtropical Pacific are retained (SPANOM); (e) as in CLIM except the SSTs are replaced with CLIM+ SSTs in the tropical Pacific (TPANOM); and (f) as in CLIM+ except the SSTs in the Atlantic are replaced with CLIM SSTs (ATLCLIM). Hashed areas in the panels indicate that the changes relative to the CLIM experiment on the grid cells are not statistically significant at the 95% confidence level (bootstrap method proposed by Murakami et al., 2013). Light gray shading in the left-hand panels indicates the SST from CLIM.

coupled or prescribed SST experiments. The fidelity of the SDAY prediction by the prescribed SST experiments gave us confidence in carrying out further sensitivity experiments with modified SSTAs.

To explore the role of the warming in the subtropical Pacific, the SSTs from CLIM+ were restored, except that the SSTs over the subtropical Pacific were replaced with those from CLIM (left-hand panel in

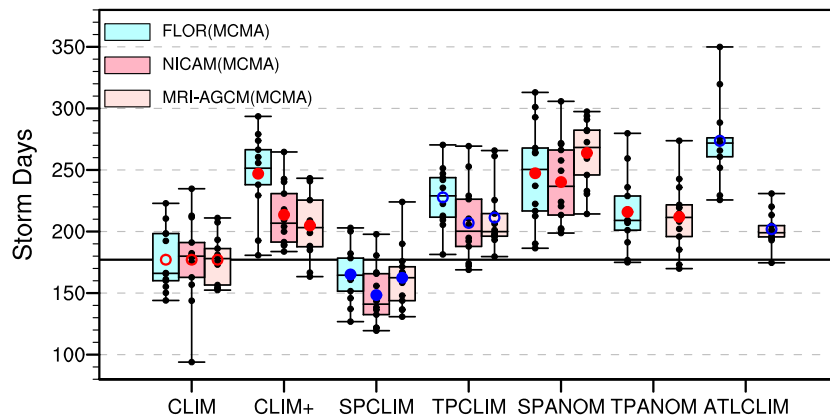


Figure 3. Boxplots for predicted storm day (SDAY) during the tropical cyclone season over the North Pacific corresponding to different prescribed sea surface temperature (SST) anomaly patterns. The red and blue dots denote the ensemble mean, while the black dots show each ensemble member. Red filled (hollow) dots indicate the mean SDAY simulated by the experiment is (not) statistically significantly different relative to that of CLIM by (not) exceeding the 95% significance level. Blue filled (hollow) dots show the same as the red dots, but for the differences relative to the CLIM+ experiment. The box represents the lower and upper quartiles, the horizontal lines in the middle show the median value, and the horizontal end lines show the lowest (highest) values. The horizontal black line represents the ensemble mean of SDAY in the CLIM experiments. Units: days. MCMA indicates that the series of experiments are based on the prescribed SSTs from FLOR's simulated climatological mean SSTs plus FLOR's predicted SST anomalies. FLOR = Forecast-Oriented Low Ocean Resolution; NICAM = Nonhydrostatic Icosahedral Atmospheric Model; MRI-AGCM = Meteorological Research Institute Atmospheric General Circulation Model.

Figure 2b). This experiment was named SPCLIM. The positive SDAY anomalies in the eastern quadrant of the WNP and CP, as shown in CLIM+, were significantly reduced and became slightly negative in the SPCLIM experiments. The basin-total SDAY values of SPCLIM were reduced markedly from those of CLIM+ (Figure 3). These results suggest that the higher SSTAs in the subtropical Pacific were the critical factor for the active 2018 TC season in the North Pacific. To investigate the influence of the tropical Pacific warming, a similar experiment to CLIM+ was conducted, except that the SSTs in the tropical Pacific were replaced with those from CLIM. This experiment was named TPCLIM (Figure 2c). The negative SDAY anomalies in the South China Sea and the Philippine Sea were found to be larger in TPCLIM than in CLIM+ (Figure 2a), indicating that the tropical CP warming was a contributing factor for the TC activity in the North Pacific, especially in the South China Sea and Philippine Sea. The simulated basin-total SDAY value in TPCLIM was slightly reduced from that of CLIM+ (Figure 3) but not exceeding the 95% significance level, because the simulated negative anomaly in the eastern Pacific, as seen in CLIM+, was replaced with a slightly positive anomaly in TPCLIM that in turn cancelled out the simulated decrease in the South China Sea and Philippine Sea.

To clarify more details on the different roles of the warmings in the subtropical and tropical Pacific, experiments similar to CLIM+ were conducted but using the CLIM+ SSTs only in the subtropical Pacific (SPANOM; Figure 2d) and tropical Pacific (TPANOM; Figure 2e). The SPANOM experiments showed that the simulated spatial pattern of SDAY anomalies was very similar to that of CLIM+, indicating that the subtropical Pacific warming alone could reproduce most of the 2018 SDAY spatial anomaly patterns. In contrast, the warming in the tropical Pacific caused a positive SDAY anomaly in the WNP and a negative SDAY anomaly in the tropical eastern North Pacific (Figure 2e). The basin-total SDAY values in the SPANOM and TPANOM experiments increased significantly ($p < 0.05$) compared with CLIM (Figure 3). Therefore, it can be concluded that the warmer SSTs in both regions played important roles for the emergence of the active 2018 TCs; however, they activated TCs at different locations: Active TCs in the CP (WNP) were mainly associated with the higher SSTs in the subtropical Pacific (tropical CP). Although the warming in the tropical CP affected more TCs in the South China Sea and the Philippine Sea, this was partially cancelled out by the slightly negative SDAY anomalies induced by the warming in the subtropical Pacific. Moreover, the negative SDAY anomaly in the tropical eastern Pacific was mainly induced by the tropical Pacific SSTA. It is further shown in Figure S4 that those changes in TC activity were associated with the location of the monsoon trough. The simulated center of the monsoon trough shifted eastward and was

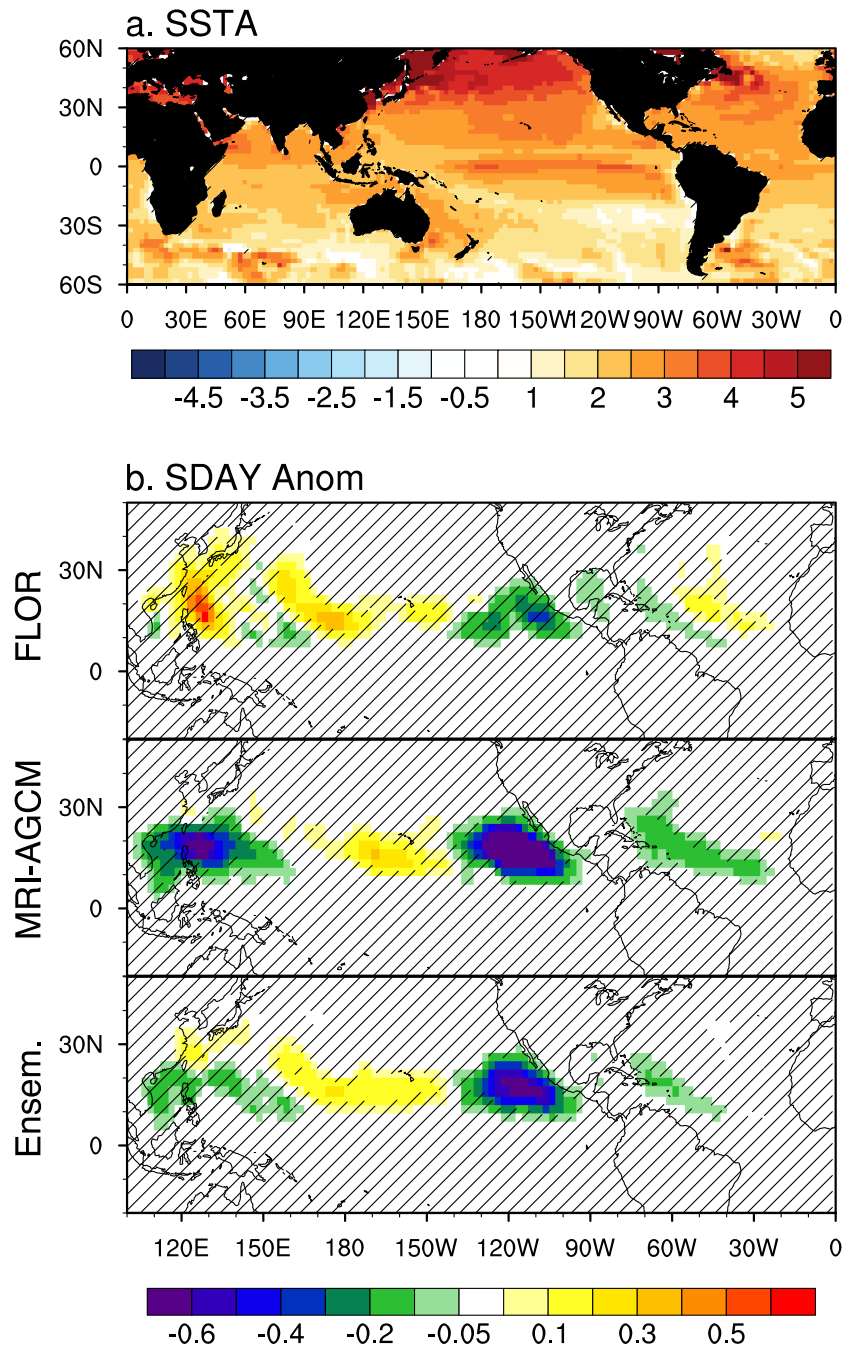


Figure 4. Projected future changes in SST and storm day during the tropical cyclone season. (a) Projected future changes in SSTs (K) simulated by the Phase 5 of the Coupled Model Intercomparison Project models under the RCP8.5 scenario (2081–2100) compared to the present-day mean state (1982–2012) and (b) projected storm day changes (days per season) between the RCP8.5 scenarios and the present-day climatological mean by FLOR, MRI-AGCM, and their ensemble mean. Hashed areas in the panels indicate the changes are not different from 0 at the 95% confidence level (bootstrap method proposed by Murakami et al., 2013). FLOR = Forecast-Oriented Low Ocean Resolution; MRI-AGCM = Meteorological Research Institute Atmospheric General Circulation Model; SST = sea surface temperature; SSTA = sea surface temperature anomaly.

located east of the tropical WNP in the SPANOM experiments relative to the CLIM experiments (Figure S4d). Therefore, more TCs were generated in the tropical CP, which in turn led to a larger SDAY value in the North Pacific owing to a longer duration. It appears that the monsoon trough did not shift

markedly in response to the tropical CP warming but intensified at the same maximum location as in the CLIM experiments (Figure S4e), leading to more TC genesis and occurrence in the South China Sea and Philippine Sea (Figure 2e). Note that a CP El Niño event triggers warming not only in the central tropical Pacific but also in the subtropical Pacific, via ocean mixed-layer dynamics (Chiang & Vimont, 2004; Lorenzo et al., 2015; Stuecker, 2018); thus, the subtropical Pacific warming observed in 2018 could have been a mixture of a positive phase of PMM and a CP El Niño event (Stuecker, 2018).

The roles of warming in the Atlantic and the warming in the WNP near Japan were also investigated, revealing that these warmings were not major factors for the 2018 active TC season in the North Pacific (see details in Text S3).

3.3. Possible Effect of Anthropogenic Forcing on the Active 2018 TC Season

The spatial pattern of the observed SSTAs for the 2018 summer (Figure 1e) is somewhat similar to the future (2081–2100) changes in SSTs projected by the models in Phase 5 of the Coupled Model Intercomparison Project under the RCP8.5 scenario, showing larger increases in SSTs in both the tropical CP and subtropical Pacific than in the rest of the world (Figure 4a). Although it is impossible to identify the proportion of the observed 2018 SSTAs that were due to an increase in anthropogenic forcing, it is possible that an increase in anthropogenic forcing might have contributed to the active 2018 TC season in the North Pacific. To investigate the potential impact of anthropogenic forcing on TC activity in the North Pacific, experiments that were similar to the idealized seasonal predictions were conducted. Projected mean future changes in SSTs by the Phase 5 of the Coupled Model Intercomparison Project models under the RCP8.5 scenario over the period 2081–2100 were superimposed onto the present-day observed climatological mean SSTs (1982–2012) along with changes in atmospheric composition projected for 2090 based on the RCP8.5 scenario (Table S1). This experiment is referred to as the RCP8.5 experiment. The RCP8.5 experiment simulated an increase in SDAY values in the CP and a decrease in the eastern Pacific relative to the CLIM experiments, with consistent results in both FLOR and MRI-AGCM (Figure 4b). However, FLOR (MRI-AGCM) showed a significant increase (decrease) in SDAY values in the WNP. This inconsistency in the WNP resulted in an opposite sign of the projected change in basin-total SDAY values in the North Pacific in the two models' results: an increase by FLOR and a decrease by MRI-AGCM, which were both statistically significant relative to the CLIM experiments (Figure S5). This inconsistency among the models highlights the considerable uncertainty in the projected future changes in SDAY in the North Pacific, especially in the WNP.

The opposite sign of the projected change in SDAY over the WNP may come from the marked differences in the changes in atmospheric stability (defined as the difference in potential temperature between 200 and 850 hPa; Figure S6b) and strength of the Indo-Pacific Walker circulation (Figures S6f and S6g). MRI-AGCM projected a large increase in atmospheric stability along with a large weakening of the Indo-Pacific Walker circulation, whereas FLOR projected a small increase in atmospheric stability and a small weakening of the Walker circulation. Owing to the significant projected decrease in upward motion at the ascending branch of the Indo-Pacific Walker circulation (i.e., 60–120°E; Figure S6g), MRI-AGCM projected larger decreases in upward vertical velocity (Figure S6a), relative humidity in the mid-troposphere (Figure S6c), and relative vorticity in the lower-troposphere (Figure S6d) in the WNP compared with FLOR. This uncertainty (or model dependency) in the sensitivity of atmospheric static stability and Walker circulations to an increase in anthropogenic forcing causes significant uncertainty in the projected future changes in TC activity in the North Pacific, especially over the WNP.

4. Summary and Uncertainty

Using a series of idealized numerical experiments, it was found that the highly active 2018 TC season in the North Pacific was driven mainly by the warming in the subtropical Pacific and secondarily by the warming in the tropical CP. However, the future climate change of TC activity in the WNP showed marked uncertainty in the different models. Therefore, it is unclear how much anthropogenic forcing impacted the occurrence of the active 2018 TC season in the North Pacific. This study highlights the importance of multimodel approaches to attribution studies owing to the uncertainty and model dependency on the effect of anthropogenic forcing to projected changes in large-scale parameters and TC activity.

Acknowledgments

The authors thank Nat Johnson and Mitch Bushuk for their suggestions and comments. This work was partly supported by the National Key R&D Program of China (2018YFC1505804) and China Scholarship Council (File 201808320271). The NICAM simulations were conducted on K Computer (Proposal hp180182) and post-processed on the data analyzer at JAMSTEC. The Earth Simulator super-computer was used for the simulations with MRI-AGCM. The data analyzed in this paper are available online (at <ftp://nomads.gfdl.noaa.gov/1p/users/Hiroyuki.Murakami/2018TC/FLOR-NICAM-MRI/>).

References

- Ashok, K., & Yamagata, T. (2009). The El Niño with a difference. *Nature*, *461*(7263), 481–484. <https://doi.org/10.1038/461481a>
- Bell, G. D., Halpert, M. S., Schnell, R. C., Higgins, R. W., Lawrimore, J., Kousky, V. E., et al. (2000). The 1999 North Atlantic and eastern North Pacific hurricane season [in “Climate Assessment for 1999”]. *Bulletin of the American Meteorological Society*, *81*(6), s1–s50. [https://doi.org/10.1175/1520-0477\(2000\)81\[s1:CAF\]2.0.CO;2](https://doi.org/10.1175/1520-0477(2000)81[s1:CAF]2.0.CO;2)
- Camargo, S. J., & Sobel, A. H. (2005). Western North Pacific tropical cyclone intensity and ENSO. *Journal of Climate*, *18*(15), 2996–3006. <https://doi.org/10.1175/JCLI3457.1>
- Chan, J. C. L. (2007). Interannual variations of intense typhoon activity. *Tellus*, *59*(4), 455–460. <https://doi.org/10.1111/j.1600-0870.2007.00241.x>
- Chang, P., Zhang, L., Saravanan, R., Vimont, D. J., Chiang, J. C. H., Ji, L., et al. (2007). Pacific meridional mode and El Niño–Southern oscillation. *Geophysical Research Letters*, *34*, L16608. <https://doi.org/10.1029/2007GL030302>
- Chiang, J. C. H., & Vimont, D. J. (2004). Analogous Pacific and Atlantic meridional modes of tropical atmosphere–ocean variability. *Journal of Climate*, *17*(21), 4143–4158. <https://doi.org/10.1175/JCLI4953.1>
- Clark, J. D., & Chu, P.-S. (2002). Interannual variation of tropical cyclone activity over the central North Pacific. *Journal of the Meteorological Society of Japan*, *80*(3), 403–418. <https://doi.org/10.2151/jmsj.80.403>
- Delworth, T. L., Broccoli, A. J., Rosati, A., Stouffer, R. J., Balaji, V., Beesley, J. A., et al. (2006). GFDL’s CM2 global coupled climate models. Part I: Formulation and simulation characteristics. *Journal of Climate*, *19*(5), 643–674. <https://doi.org/10.1175/JCLI3629.1>
- Delworth, T. L., Rosati, A., Anderson, W., Adcroft, A. J., Balaji, V., Benson, R., et al. (2012). Simulated climate and climate change in the GFDL CM2.5 high-resolution coupled climate model. *Journal of Climate*, *25*(8), 2755–2781. <https://doi.org/10.1175/JCLI-D-11-00316.1>
- Duan, W., & Wei, C. (2013). The ‘spring predictability barrier’ for ENSO predictions and its possible mechanism: Results from a fully coupled model. *International Journal of Climatology*, *33*(5), 1280–1292. <https://doi.org/10.1002/joc.3513>
- Gao, S., Zhu, L., Zhang, W., & Chen, Z. (2018). Strong modulation of the Pacific meridional mode on the occurrence of intense tropical cyclones over the western North Pacific. *Journal of Climate*, *31*(19), 7739–7749. <https://doi.org/10.1175/JCLI-D-17-0833.1>
- Hong, C.-C., Li, Y.-H., Li, T., & Lee, M.-Y. (2011). Impacts of central Pacific and eastern Pacific El Niño on tropical cyclone tracks over the western North Pacific. *Geophysical Research Letters*, *38*, L16712. <https://doi.org/10.1029/2011GL048821>
- Knapp, K. R., Kruk, M. C., Levinson, D. H., Diamond, H. J., & Neumann, C. J. (2010). The international best track archive for climate stewardship (IBTrACS): Unifying tropical cyclone best track data. *Bulletin of the American Meteorological Society*, *91*(3), 363–376. <https://doi.org/10.1175/2009BAMS2755.1>
- Kobayashi, S., Ota, Y., Harada, Y., Ebata, A., Moriwa, M., Onoda, H., et al. (2015). The JRA-55 reanalysis: General specifications and basic characteristics. *Journal of the Meteorological Society of Japan*, *93*(1), 5–48. <https://doi.org/10.2151/jmsj.2015-001>
- Lorenzo, E. D., Liguori, G., Schneider, N., Furtado, J. C., Anderson, B. T., & Alexander, M. A. (2015). ENSO and meridional modes: A null hypothesis for Pacific climate variability. *Geophysical Research Letters*, *42*, 9440–9448. <https://doi.org/10.1002/2015GL066281>
- Miura, H., Satoh, M., Nasuno, T., Noda, A. T., & Oouchi, K. (2007). A Madden-Julian oscillation event realistically simulated by a global cloud-resolving model. *Science*, *318*(5857), 1763–1765. <https://doi.org/10.1126/science.1148443>
- Mizuta, R., Yoshimura, H., Murakami, H., Matsueda, M., Endo, H., Ose, T., et al. (2012). Climate simulations using the improved MRI-AGCM with 20-km grid. *Journal of the Meteorological Society of Japan*, *90A*, 233–258. <https://doi.org/10.2151/jmsj.2012-A12>
- Murakami, H., Levin, E., Delworth, T. L., Gudgel, R., & Hsu, P.-C. (2018). Dominant effect of relative tropical Atlantic warming on major hurricane occurrence. *Science*, *362*(6416), 794–799. <https://doi.org/10.1126/science.aat6711>
- Murakami, H., Mizuta, R., & Shindo, E. (2012). Future changes in tropical cyclone activity projected by multi-physics and multi-SST ensemble experiments using the 60-km-mesh MRI-AGCM. *Climate Dynamics*, *39*(9–10), 2569–2584. <https://doi.org/10.1007/s00382-011-1223-x>
- Murakami, H., Vecchi, G. A., Delworth, T. L., Wittenberg, A. T., Underwood, S., Gudgel, R., et al. (2017). Dominant role of subtropical Pacific warming in extreme eastern Pacific hurricane seasons: 2015 and the future. *Journal of Climate*, *30*(1), 243–264. <https://doi.org/10.1175/JCLI-D-16-0424.1>
- Murakami, H., Wang, B., Li, T., & Kitoh, A. (2013). Projected increase in tropical cyclones near Hawaii. *Nature Climate Change*, *3*(8), 749–754. <https://doi.org/10.1038/nclimate1890>
- Murakami, H., Wang, Y., Yoshimura, H., Mizuta, R., Sugi, M., Shindo, E., et al. (2012). Future changes in tropical cyclone activity projected by the new high-resolution MRI-AGCM. *Journal of Climate*, *25*(9), 3237–3260. <https://doi.org/10.1175/JCLI-D-11-00415.1>
- Nakano, M., Sawada, M., Nasuno, T., & Satoh, M. (2015). Intraseasonal variability and tropical cyclogenesis in the western North Pacific simulated by a global nonhydrostatic atmospheric model. *Geophysical Research Letters*, *42*, 565–571. <https://doi.org/10.1002/2014GL062479>
- Patricola, C. M., Camargo, S. J., Klotzbach, P. J., Saravanan, R., & Chang, P. (2018). The influence of ENSO flavors on western North Pacific tropical cyclone activity. *Journal of Climate*, *31*(14), 5395–5416. <https://doi.org/10.1175/JCLI-D-17-0678.1>
- Rayner, N. A., Parker, D. E., Horton, E. B., Folland, C. K., Alexander, L. V., Rowell, D. P., et al. (2003). Global analyses of sea surface temperature, sea ice, and night marine air temperature since the late nineteenth century. *Geophysical Research Letters*, *108*(D14), 4407. <https://doi.org/10.1029/2002JD002670>
- Satoh, M., Matsuno, T., Tomita, H., Miura, H., Nasuno, T., & Iga, S. (2008). Nonhydrostatic Icosahedral Atmospheric Model (NICAM) for global cloud resolving simulations. *Journal of Computational Physics*, *227*(7), 3486–3514. <https://doi.org/10.1016/j.jcp.2007.02.006>
- Satoh, M., Tomita, H., Yashiro, H., Miura, H., Kodama, C., Seiki, T., et al. (2014). The Non-hydrostatic icosahedral atmospheric model: Description and development. *Progress in Earth and Planetary Science*, *1*(1), 1–32. <https://doi.org/10.1186/s40645-014-0018-1>
- Stuecker, M. F. (2018). Revisiting the Pacific meridional mode. *Scientific Reports*, *8*(1), 3216. <https://doi.org/10.1038/s41598-018-21537-0>
- Tropical Cyclone Guidance Project (2019). available online at <http://hurricanes.ral.ucar.edu/repository/>
- Vecchi, G. A., Delworth, T., Gudgel, H., Kapnick, S., Rosati, A., Wittenberg, A. T., et al. (2014). On the seasonal forecasting of regional tropical cyclone activity. *Journal of Climate*, *27*, 7994–8016. <https://doi.org/10.1175/JCLI-D-14-00158.1>
- Wang, B., & Chan, J. C. L. (2002). How strong ENSO events affect tropical storm activity over the western North Pacific. *Journal of Climate*, *15*(13), 1643–1658. [https://doi.org/10.1175/1520-0442\(2002\)015<1643:HSEAT>2.0.CO;2](https://doi.org/10.1175/1520-0442(2002)015<1643:HSEAT>2.0.CO;2)
- Wang, B., Yang, Y., Ding, Q.-H., Murakami, H., & Huang, F. (2010). Climate control of the global tropical storm days (1965–2008). *Geophysical Research Letters*, *37*, L07704. <https://doi.org/10.1029/2010GL042487>
- Yamada, Y., Kodama, C., Satoh, M., Nakano, M., Nasuno, T., & Sugi, M. (2019). High-resolution ensemble simulations of intense tropical cyclones and their internal variability during the El Niños of 1997 and 2015. *Geophysical Research Letters*, *46*(13), 7592–7601. <https://doi.org/10.1029/2019GL082086>

- Yamada, Y., Satoh, M., Sugi, M., Kodama, C., Noda, A. T., Nakano, M., & Nasuno, T. (2017). Response of tropical cyclone activity and structure to global warming in a high-resolution global nonhydrostatic model. *Journal of Climate*, *30*(23), 9703–9724. <https://doi.org/10.1175/JCLI-D-17-0068.1>
- Yoshida, K., Sugi, M., Mizuta, R., Murakami, H., & Ishii, M. (2017). Future changes in tropical cyclone activity in high-resolution large-ensemble simulations. *Geophysical Research Letters*, *44*, 9910–9917. <https://doi.org/10.1002/2017GL075058>
- Zhang, W., Vecchi, G. A., Murakami, H., Villarini, G., & Jia, L. (2016). The Pacific meridional mode and the occurrence of tropical cyclones in the western North Pacific. *Journal of Climate*, *29*(1), 381–398. <https://doi.org/10.1175/JCLI-D-15-0282.1>

References From the Supporting Information

- Cao, X., Chen, S., Chen, G., & Wu, R. (2016). Intensified impact of northern tropical Atlantic SST on tropical cyclogenesis frequency over the western North Pacific after the late 1980s. *Advances in Atmospheric Sciences*, *33*(8), 919–930. <https://doi.org/10.1007/s00376-016-5206-z>
- Gao, S., Chen, Z., & Zhang, W. (2018). Impacts of tropical North Atlantic SST on western North Pacific landfalling tropical cyclones. *Journal of Climate*, *31*(2), 853–862. <https://doi.org/10.1175/JCLI-D-17-0325.1>
- Kucharski, K., Kang, I.-S., Farneti, R., & Feudale, L. (2011). Tropical Pacific response to 20th century Atlantic warming. *Geophysical Research Letters*, *38*, L03702. <https://doi.org/10.1029/2010GL046248>
- Yu, J., Li, T., Tan, Z., & Zhu, Z. (2016). Effects of tropical North Atlantic SST on tropical cyclone genesis in the western North Pacific. *Climate Dynamics*, *46*(3–4), 865–877. <https://doi.org/10.1007/s00382-015-2618-x>
- Zhang, S., & Rosati, A. (2010). An inflated ensemble filter for ocean data assimilation with a 440 biased coupled GCM. *Monthly Weather Review*, *138*(10), 3905–3931. <https://doi.org/10.1175/2010MWR3326.1>